Electronic Supplementary Material (ESI) for Chemical Communications
This journal is © The Royal Society of Chemistry 2014

Supporting Information

Excited-state electronic couplings in 1,3-butadiyne-bridged Zn(II)porphyrin dimer and trimer

Sangsu Lee,[a] *Heejae Chung,*[a] *Sumito Tokuji,*[b] *Hideki Yorimitsu,*[b] *Atsuhiro Osuka**[b] *and Dongho Kim**[a]

[a] Department of Chemistry, Yonsei University, Seoul 120-749, Korea. Fax: 82-2-2123-2436; Tel: 82-2-2123-2652; E-mail: dongho@yonsei.ac.kr

[b] Department of Chemistry and Graduate School of Science, Kyoto University, Sakyo-ku, Kyoto 606-8502, Japan. Fax: 81-75-753-3970; Tel: 81-75-753-4008; E-mail: osuka@kuchem.kyoto-u.ac.jp

This journal is © The Royal Society of Chemistry 2014

Contents

1. Experimental Details

2. Theoretical Calculations

3. Supporting Information

Table S1. List of parameters measured in steady-state absorption and emission and time-resolved fluorescence spectroscopies

Table S2. Decay parameters measured in femtosecond transient absorption anisotropy

Table S3. Decay parameters measured in pump-power dependent femtosecond transient absorption

Table S4. Parameters of Förster-type resonance energy transfer calculation

Figure S1. Picosecond time-resolved fluorescence decay profiles

Figure S2. Steady-state fluorescence excitation anisotropy

Figure S3. Picosecond time-resolved fluorescence anisotropy decay profiles

Figure S4. Femtosecond transient absorption spectrum of **D** and **T**

Figure S5. Femtosecond time-resolved fluorescence anisotropy and transient absorption anisotropy decay profiles of **M**

Figure S6. Fluorescence lifetime distributions of **D** and **T** at single-molecule level

Figure S7. Fluorescence intensity trajectories (FITs) and corresponding spectra of **D** and **T**

Figure S8. Frontier molecular orbitals of **D** and **T**

4. References

1. Experimental Details

Sample Preparation. The details in synthesis, characterization, and X-ray crystallographic analysis of **D** and **T** are described elsewhere.[1] X-Ray data were taken at –180 °C with a Rigaku RAXIS-RAPID diffraction by using graphite monochromated Cu-Ka radiation (? = 1.54187 Å). The structures were solved by direct method. Toluene was distilled from CaH2. THF and 1,4-dioxane were purified by passing through a neutral alumina column under N2. ZnTPP (with low chlorine) and toluene (HPLC grade) were purchased from Aldrich and used without further purification.

Steady-State Absorption and Emission. Steady-state UV-vis absorption spectra were recorded on a commercial spectrometer (Cary5000, Varian). Fluorescence spectra were measured by a spectrophotometer (FL2500, Hitachi) and spectral sensitivity were corrected with the comparison of the well-known chromophores such as rhodamine and coumarin dyes.[2] For the steady-state fluorescence excitation anisotropy measurement, Glan laser and sheet polarizers were added into the excitation and monitoring paths, respectively. The calculation of anisotropy at specific monitoring wavelength (λ_{em}) as a function of excitation wavelength (λ_{ex}) was the given by

$$r(\lambda_{ex}) = [\ I_{VV}(\lambda_{ex}) - GI_{VH}(\lambda_{ex})\ ] / [\ I_{VV}(\lambda_{ex}) + 2GI_{VH}(\lambda_{ex})\ ] \quad (1)$$

where $I_{VV}(\lambda_{ex})$ (or $I_{VH}(\lambda_{ex})$) is the fluorescence intensity with the photoexcitation at λ_{ex} when the excitation light is vertically polarized and only the vertically (or horizontally) polarized portion of the fluorescence is detected, and the first and second subscripts represent excitation and detection polarizations, respectively. The factor of correction factor G is defined by [$I_{HV}(\lambda_{em})$ / $I_{HH}(\lambda_{em})$], which is equal to the ratio of the sensitivity of the detection system for vertically and horizontally polarized light at given emission wavelength λ_{em}. Experimental G value was measured to be around 1.7 in our instrument. All steady-state measurements were carried out by using a quartz cuvette with a pathlength of 1 cm at ambient temperatures.

Picosecond Time-resolved Fluorescence. Time-resolved fluorescence decays were obtained by using a time-correlated single-photon counting (TCSPC) technique. A mode-locked Ti:sapphire oscillator (MaiTai-BB, Spectra Physics) were used as a excitation light source, which provide a fwhm (full width at half maximun) of 80 fs with a high repetition rate of 80 MHz. In order to minimize artifacts such as thermal lensing and accumulation effect, repetition rate was reduced down to 800 kHz using a home-made acousto-optic pulse selector. The picked fundamental pulses were frequency doubled by a 1 mm of thickness of BBO nonlinear crystal (Eksma). The fluorescence was collected by a microchannel plate photomultiplier (MCP-PMT, R3809U-51, Hamamatsu) with a thermoelectric cooler (C4878, Hamamatsu). Time-resolved fluorescence signals were calculated by a TCSPC board (SPC-130, Becker

& Hickel GmbH). The overall instrumental response function (IRF) was determined to be less than 30 ps (fwhm) in all spectral regions. A polarization of photoexcitation pulses was set to vertical to the laboratory frame by both a half-wave retarder and Glan laser polarizer and sheet polarizers were used in fluorescence collection path at magic angle (54.7°) to obtain polarization independent population decays. Time-resolved fluorescence anisotropy was obtained by changing the detection polarization on the fluorescence path to parallel or perpendicular to the polarization of the excitation pulses. The calculation of anisotropy decay at specific monitoring wavelength was the followed by

$$r(t) = [\, I_{VV}(t) - GI_{VH}(t) \,] / [\, I_{VV}(t) + 2GI_{VH}(t) \,] \qquad (2)$$

where $I_{VV}(t)$ (or $I_{VH}(t)$) is the fluorescence decay when the excitation light is vertically polarized and only the vertically (or horizontally) polarized portion of the fluorescence is detected, and the first and second subscripts represent excitation and detection polarizations, respectively. The factor of correction factor G is defined by [$I_{HV}(t)$ / $I_{HH}(t)$], which is equal to the ratio of the sensitivity of the detection system for vertically and horizontally polarized light at specific monitoring wavelength. Experimental G values were measured to be around 1.12 in our instrument.

Femtosecond Transient Absorption. Dual-beam femtosecond time-resolved transient absorption (TA) spectrometer consisted of two independently-tunable home-made optical parametric amplifiers (OPA) pumped by a regeneratively amplified Ti:sapphire laser system (Hurricane-X, Spectra-Physics) operating at 2 kHz repetition rate and an optical detection system.[3] The OPA was based on non-collinearly phase-matching geometry, which was easily color-tuned by controlling optical delay between white light continuum seed pulses (450-1400 nm) and visible pump pulses (400 nm) produced by using sapphire window and BBO crystal, respectively. The generated visible OPA pulses had a pulse width of ~ 35 fs and an average power of 5 mW at 2 kHz repetition rate in the range 500-700 nm after fused-silica prism compressor. Two OPA pulses were used as the pump and probe pulses, respectively, for TA measurement. The probe beam was split into two parts. The one part of the probe beam was overlapped with the pump beam at the sample to monitor the transient (signal), while the other part of the probe beam was passed through the sample without overlapping the pump beam to compensate the fluctuation of probe beam. The time delay between pump and probe beams was carefully controlled by making the pump beam travel along a variable optical delay (ILS250, Newport). To obtain the time-resolved transient absorption difference signal at specific wavelength, the monitoring wavelength was selected by using a narrow interference filter (FWHM ~10 nm). By chopping every another pump pulses at 1.5 kHz, the modulated probe pulses as well as the reference pulses were detected by two separate photodiodes (Femtowatt Photoreceiver, New Focus). The modulated signals of the probe pulses were measured by a gated-integrator (SR250, SRS) and a lock-in amplifier (DSP7265, EG&G) and stored in a personal

computer for further signal processing. The polarization angle between pump and probe beam was set to magic angle (54.7°) in order to prevent polarization-dependent signals. In general experimental conditions, time-resolutions of less than 60 fs were achieved. For time-resolve transient absorption anisotropy (TAA) measurement, both $I_{//}(t)$ and $I_{\perp}(t)$ signals were collected simultaneously by combination of polarizing beam-splitter cube and dual lock-in amplifiers as following equation;

$$r(t) = [\ I_{//}(t) - I_{\perp}(t)\ ] / [\ I_{//} + 2I_{\perp}(t)\ ] \quad (3)$$

where $I_{//}(t)$ and $I_{\perp}(t)$ represent TA signals with the polarization of the pump and probe pulses being mutually parallel and perpendicular respectively. This equation was also applied to the femtosecond fluorescence anisotropy measurement. The pump pulse was set to vertical polarization and that of probe pulse was set to 45° with respect to the pump pulse by using Glan-laser polarizers and half-wave plates. After the probe pulse passes through the sample cell, it was split by polarizing beam-splitter cube and then detected by two separate photodiodes. Two gated-integrators and two lock-in amplifiers record the signal simultaneously within a single scan. As a standard anisotropy measurement showed a clean single exponential decay with reorientational relaxation times of 122.1 ± 0.3 ps and the initial anisotropy r_0 value of 0.39 ± 0.02 for rhodamine 6G dye in methanol, which are well-matched in other reference.[4] For all TA and TAA measurements, thin absorption cells with a path length of 2mm and 500 μm, respectively, were used.

2. Theoretical Calculations

Quantum mechanical calculations were performed by the Gaussian09 program suite installed on supercomputer (KISTI).[5] Geometry optimizations were carried out by the density functional theory (DFT) method with the Becke's three-parameter hybrid exchange functional and the Lee-Yang-Parr correlation functional (B3LYP),[6, 7] employing a basis set containing 6-31G(d) for all atoms.[8] The X-ray crystallographic structures were used as initial geometries for geometry optimization.[1] To simulate the ground-state absorption spectra, we used time-dependent (TD) DFT calculations with the same functional and basis set as used in the geometry optimization.[9] Electron density difference maps (EDDM) were calculated by GAUSSSUM 2.2 program package using results of TDDFT.[10] All computational analyses were carried out omitting tertiary-butyl substituents in all phenyl groups to reduce computational cost since substituent effects on electronic structures of porphyrin rings by additional substituents far from porphyrin skeleton usually negligible in these systems.[11]

3. Supporting Information

Table S1 List of parameters measured in steady-state absorption and emission and time-resolved fluorescence spectroscopies in toluene

Steady-State Absorption, Emission and Time-resolved Fluorescence Lifetimes in toluene							
Sample	λ_{abs}[a](ε($10^3 M^{-1}cm^{-1}$)) (nm)	λ_{em}[b](nm)	Φ_F[c]	τ_F[d] (ns)	k_{rad}[e](s^{-1})	k_{nonrad}[f](s^{-1})	τ_R[g] (ns)
M	423(574), 549(25), 587(4)	597, 646	0.033	1.99±0.02	1.7 x 10^7	4.9 x 10^8	0.12±0.01
D	441(300), 502(190), 557(40), 580(35), 604(37), 640(8)	615, 657, 732, 770	0.025	2.37±0.01	1.1 x 10^7	4.1 x 10^8	0.78±0.04
T	453(372), 491(507), 535(44) 562(86), 580(105), 603(112)	610, 630, 693, 731	0.059	2.09±0.01	2.8 x 10^7	4.5 x 10^8	1.39±0.13

[a]Peak maxima of steady-state UV-Vis absorption spectra. [b]Peak maxima of steady-state fluorescence spectra. Excitation wavelengths were 420(**M**), 441(**D**) and 491 nm (**T**), respectively. [c]Fluorescence quantum yields. [d]Fluorescence lifetimes measured by TCSPC with the excitation wavelength of 420(**M**), 450(**D**, **T**) nm for all Q-states. [e]Radiative decay rate constants were calculated by using fluorescence quantum yields[c] and fluorescence lifetimes[d]. [f]Non-radiative decay rate constants were calculated by fluorescence quantum yields[c] and fluorescence lifetimes[d]. [g] Rotational reorientation times measured by TCSPC anisotropy.

Table S2 Decay parameters measured in femtosecond transient absorption anisotropy in toluene.

	Fitted decay times (fs) and Anisotropy value						
	λ_{pump}	λ_{probe}	r_0	r_1	τ_1	τ_2	r_{inf}
M	413nm	432nm	0.76	0.48	83	185	0.11
	550nm	500nm	0.25	-	120	-	0.06
D	610nm	530nm	-	-0.11	-	457	-0.14
T			-	0.06	-	468	0.025

Anisotropy decay time constants were measured by transient absorption anisotropy method except for the B-state of **M**, which were determined by fluorescence up-conversion and anisotropy measurements. The second time constants were fixed by the fluorescence lifetimes from the TCSPC data. Anisotropy decays were fitted by $C_1[\exp(-t/\tau_1)] + C_2[\exp(-t/\tau_2)] + r_{inf}$, where $r_0 = C_1 + C_2 + r_{inf}$ and $r_1 = C_2 + r_{inf}$. The infinite anisotropy value (r_{inf}) indicates the last value in the time window employed in our measurement.

Table S3 Decay parameters measured by pump-power dependent femtosecond transient absorption in toluene.

	Fitted decay times (ps)					
	Pump power	λ_{pump}	λ_{probe}	τ_1	τ_2	τ_{hop}
T	4mW	460nm	655nm	1.2 (37.8%)	2100(62.2%)	3.6
	2mW			1.2 (19.7%)	2100(80.3%)	
	1mW			1.2 (12.5%)	2100(87.5%)	
	0.5mW			1.2 (9.7%)	2100(90.3%)	

Table S4 Parameters of Förster-type resonance energy transfer calculation

Parameter of Förster resonance energy transfer calculation								
Sample	τ_F[a] (ns)	r[b]	κ[c]	n[d]	Φ_F[e]	R_0[f]	k_T[g] (s^{-1})	τ[h] (ps)
D	1.99±0.02	13.586	-2	1.496	0.025	29.54	4.45×10^{10}	22
T	1.99±0.02	14.987	-0.43205	1.496	0.059	26.78	1.56×10^{10}	64

[a]Fluorescence lifetime. [b]Donor-acceptor distance. [c]Orientation factor. [d]Refractive index of toluene. [e]Fluorescence quantum yields. [f]Förster radius. [g]The rate of energy transfer. [h]Calculated Förster-type resonance energy transfer time.

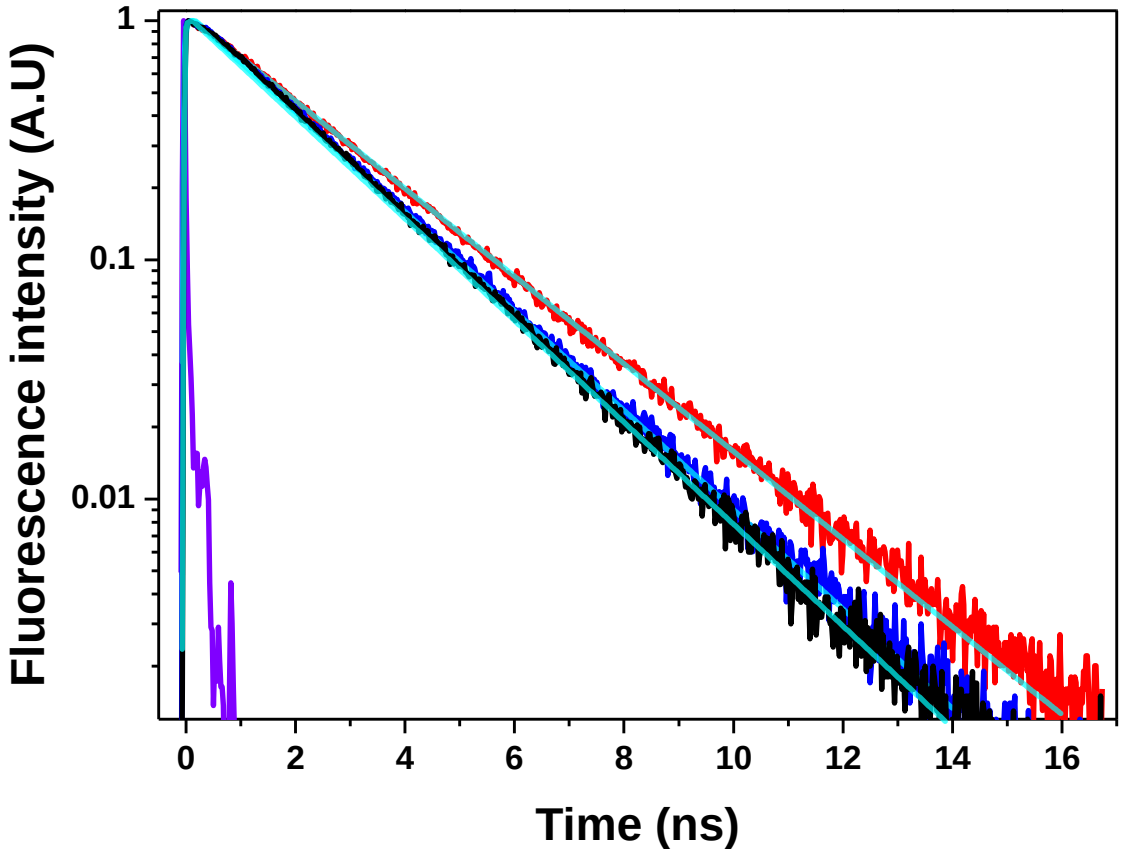

Fig. S1 Time-resolved fluorescence decay profiles of **M** (black line), **D** (red line) and **T** (blue line) in toluene obtained by using TCSPC technique with the photoexcitation at 420 (**M**), 450 (**D**, **T**) nm with the best fit curves (cyan lines). Temporal profile for instrumental response function is plotted for comparison (violet line, fwhm of ~ 30 ps).

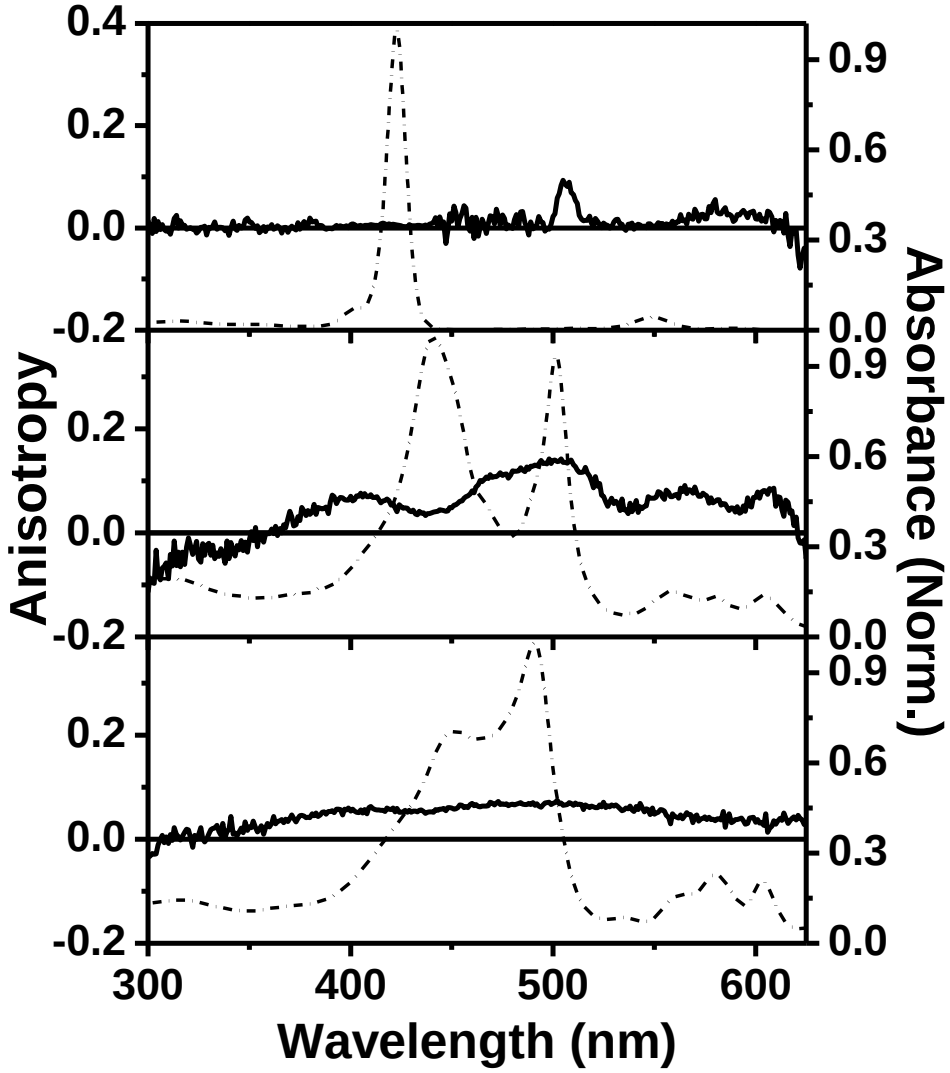

Fig. S2 Steady-state fluorescence excitation anisotropy (solid lines) of **M** (top), **D** (middle), **T** (bottom) in toluene. The fluorescence was monitored at 646 (**M**), 733 (**D**) and 630 nm (**T**), respectively.

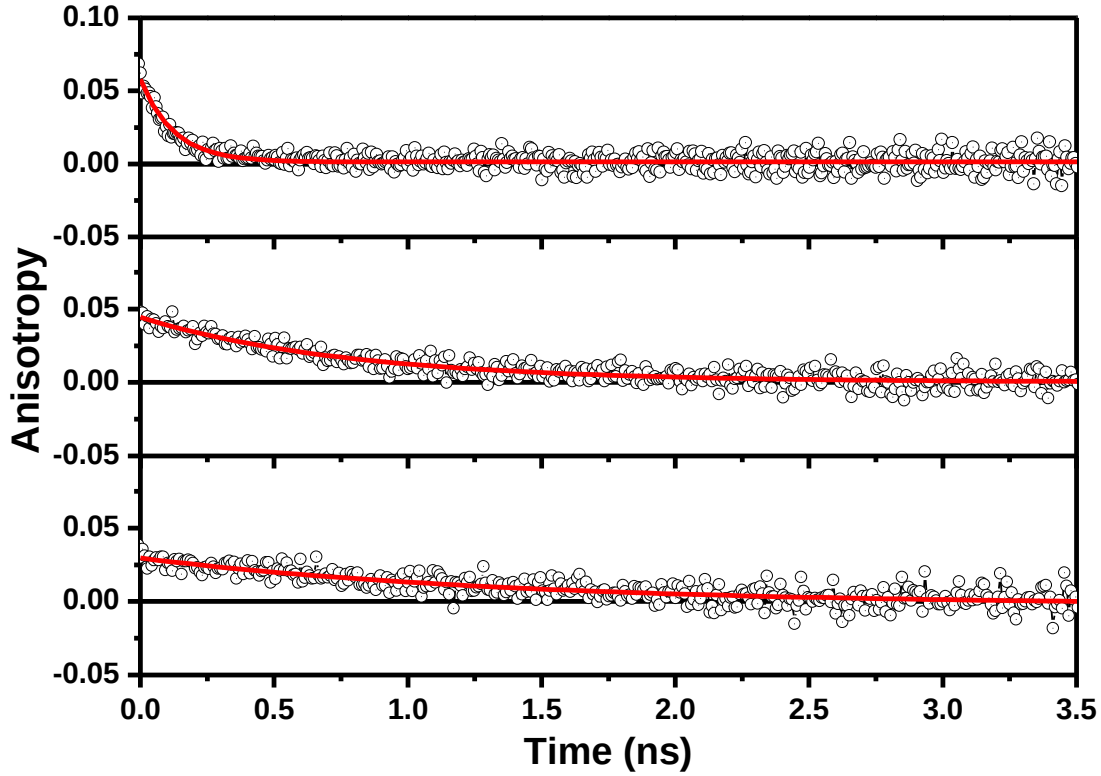

Fig. S3 Time-resolved fluorescence anisotropy decay profiles (open circles) of **M** (top), **D** (middle), and **T** (bottom) in toluene with the photoexcitation at 420 (**M**), 450 (**D**, **T**) nm with the best fitting curves (red lines). All data were fitted by using single exponential decay function. The fitted decay time constants correspond to rotational reorientation times.

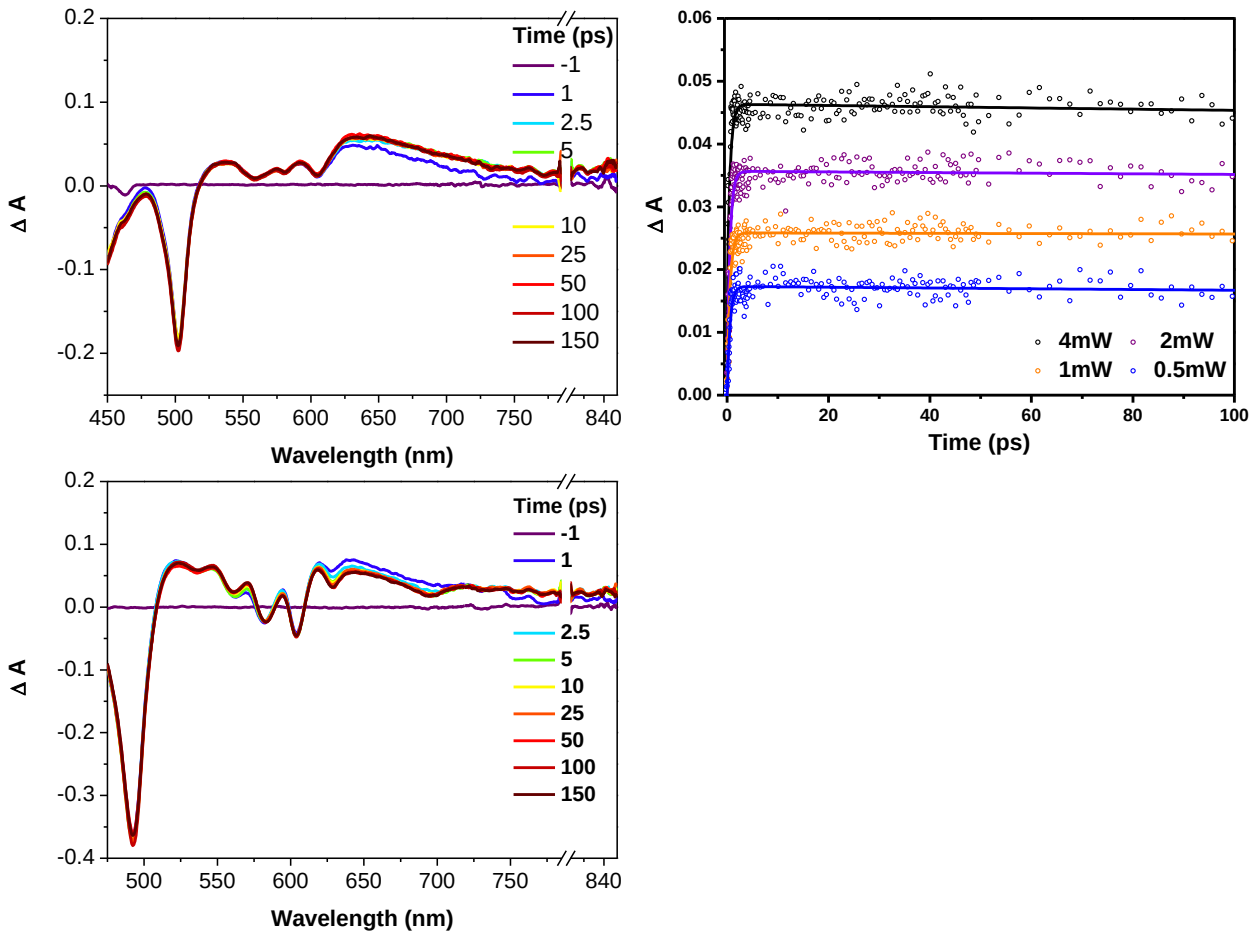

Fig. S4 Femtosecond transient absorption spectra and pump-power dependence of **D** (top) and femtosecond transient absorption spectra of **T** (bottom) in toluene obtained with the photoexcitation at 460 nm.

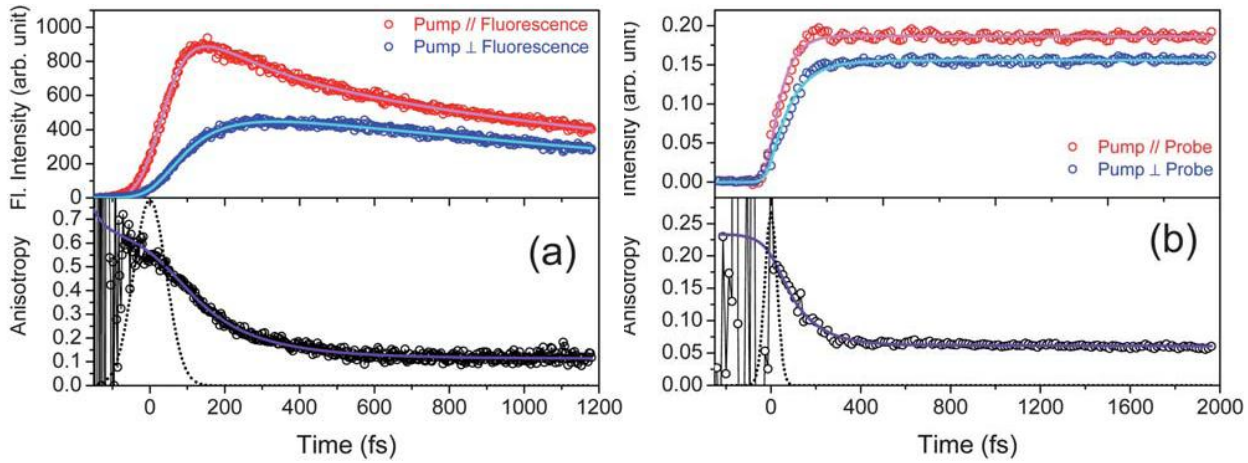

Fig. S5 (a) Time-resolved fluorescence (top) and anisotropy (bottom) decay profiles B-state of **M** in toluene obtained by using fluorescence up-conversion with the photoexcitation at 413 nm and monitored at 432 nm. (b) Time-resolved transient absorption (top) and anisotropy (bottom) decay profiles of Q-state of **M** in toluene with the photoexcitation at around 550 nm region and probed at 500 nm (photo-induced absorption). Solid lines correspond to the best fitting curves by least-square nonlinear fitting with deconvolution with instrumental response function.

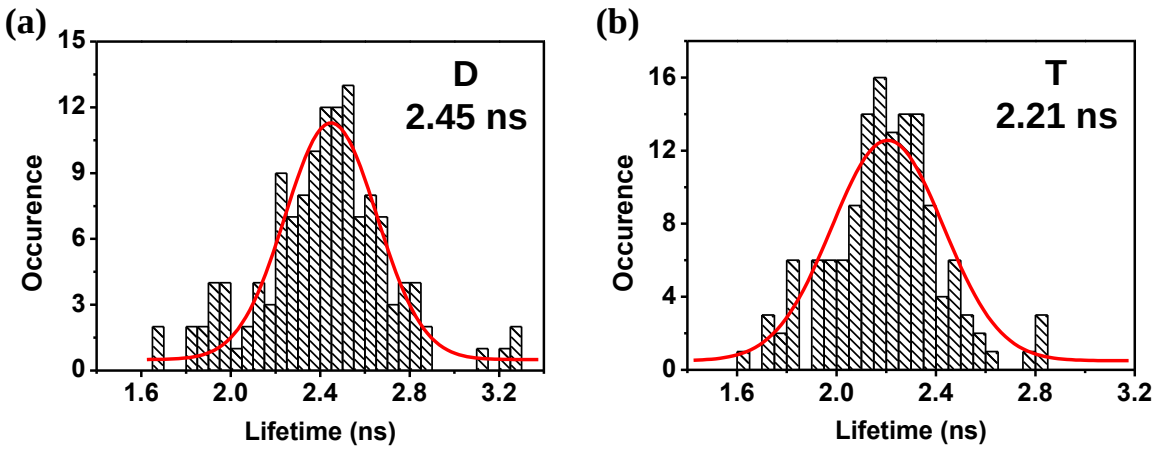

	1 step	2 step	3 step
D	77 % (103/134)	23 % (31/134)	
T	71 % (99/139)	24 % (29/139)	5 % (11/139)

Fig. S6 Fluorescence lifetime distributions of **D** (left) and **T** (right) at the first emissive level. **D** shows one- and two-step photobleaching behavior and **T** shows one-, two- and three-step photobleaching behavior. The histograms were constructed by collecting more than 100 single-molecule datasets for each molecule. The solid lines correspond to the fitted Gaussian curves.

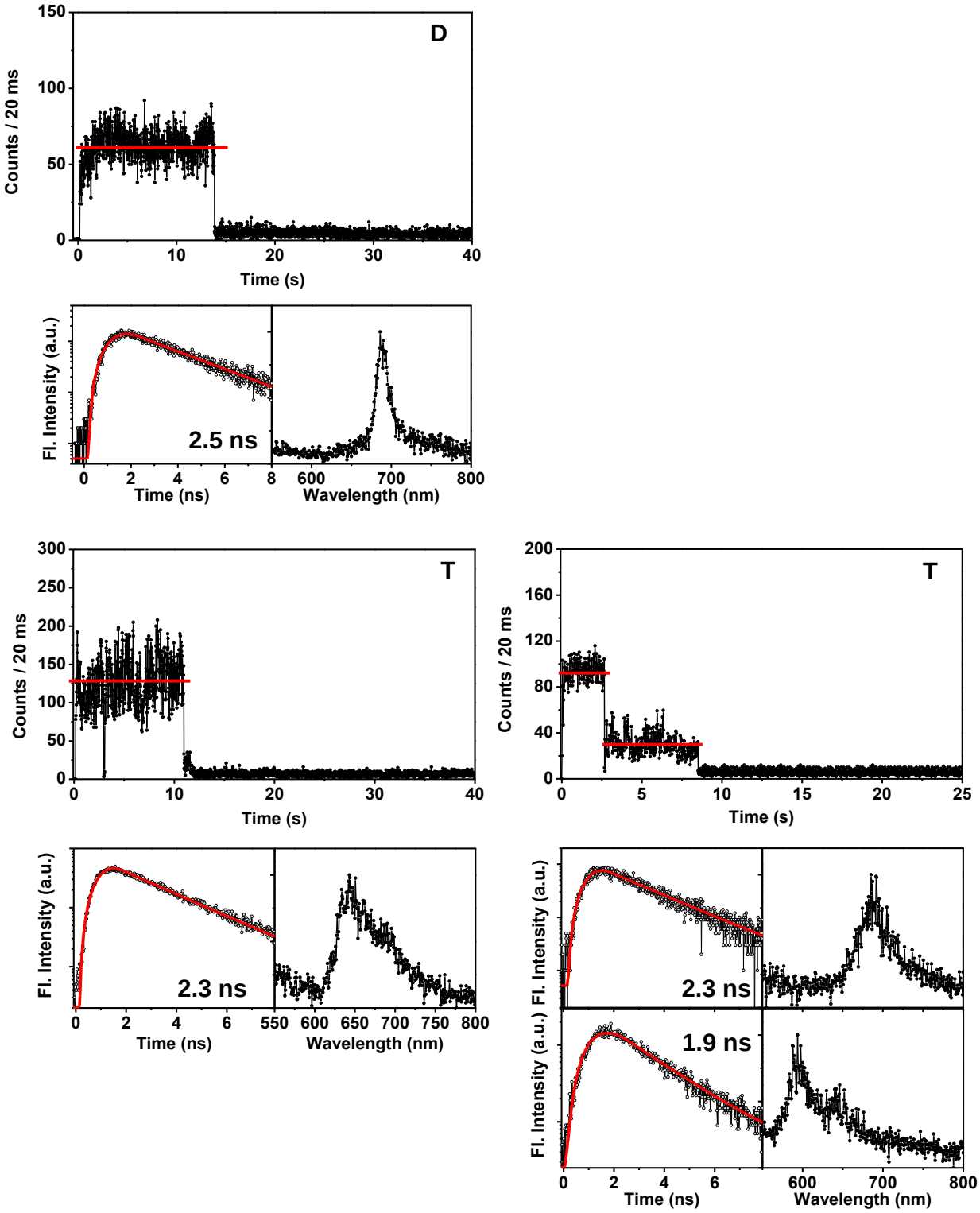

Fig. S7 Representative fluorescence intensity trajectories (FITs) and corresponding spectra of **D** (top) and **T** (bottom).

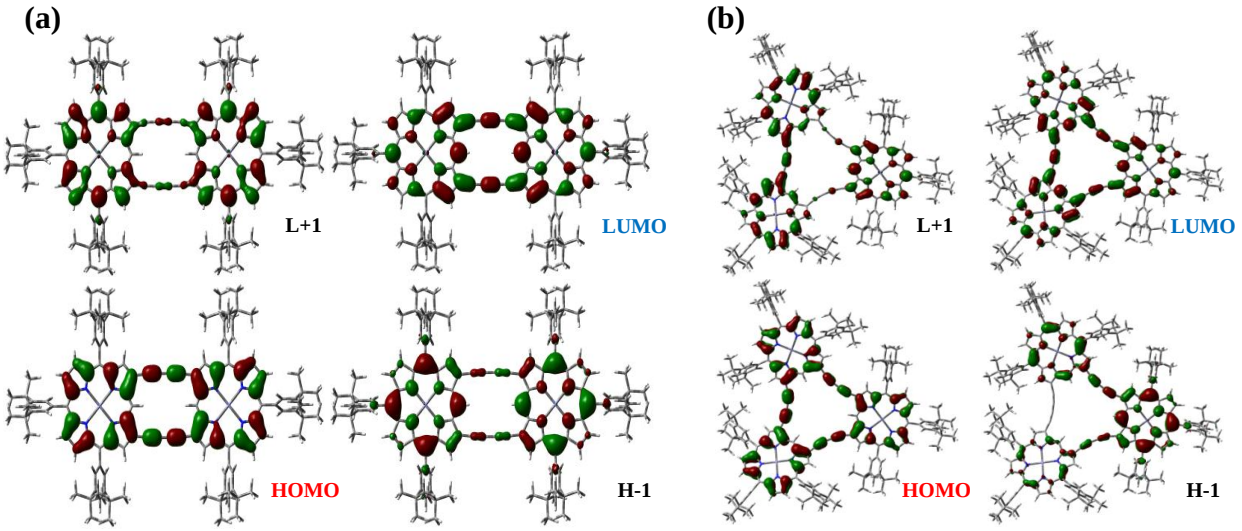

Fig. S8 Frontier molecular orbitals of (a) **D** and (b) **T**.

4. References

1. S. Tokuji, H. Yorimitsu and A. Osuka, *Angew. Chem. Int. Ed.* 2012, **51**, 12357-12361.
2. J. Lakowicz, *Principles of Fluorescence Spectroscopy*, Kluwer Academic/Plenum Publishers, New York, Boston, Dordrecht, London, Moscow, 1999.
3. M. C. Yoon, S. Cho, P. Kim, T. Hori, N. Aratani, A. Osuka and D. Kim, *J. Phys. Chem. B*, 2009, **113**, 15074-15082.
4. L. A. Philips, S. P. Webb, S. W. Yeh and J. H. Clark, J. Phys. Chem., 1985, **89**, 17-19.
5. M. J. Frisch, G. W. Trucks, H. B. Schlegel, G. E. Scuseria, M. A. Robb, J. R. Cheeseman, V. G. Zakrzewski, J. A. J. Montgomery, R. E. Stratmann, J. C. Burant, S. Dapprich, J. M. Millam, A. D. Daniels, K. N. Kudin, M. C. Strain, O. Farkas, J. Tomasi, V. Barone, M. Cossi, R. Cammi, B. Mennucci, C. Pomelli, C. Adamo, S. Clifford, J. Ochterski, G. A. Petersson, P. Y. Ayala, Q. Cui, K. Morokuma, D. K. Malick, A. D. Rabuck, K. Raghavachari, J. B. Foresman, J. Cioslowski, J. V. Ortiz, B. B. Stefanov, G. Liu, A. Liashenko, P. Piskorz, I. Komaromi, R. Gomperts, R. L. Martin, D. J. Fox, T. Keith, M. A. Al-Laham, C. Y. Peng, A. Nanayakkara, C. Gonzalez, M. Challacombe, P. M. W. Gill, B. G. Johnson, W. Chen, M. W. Wong, J. L. Andres, M. Head-Gordon, E. S. Replogle and J. A. Pople, Gaussian, Inc., Wallingford CT, 2004.
6. A. D. Becke, *J. Chem. Phys.* 1993, **98**, 5648-5652
7. C. Lee, W. Yang and R. G. Parr, *Phys. Rev. B*. 1988, **37**, 785-789.
8. R. Ditchfield, W. J. Hehre and J. A. Pople, *J. Chem. Phys.* 1971, **54**, 724-728.
9. R. Bauernschmitt and R. Ahlrichs, *Chem. Phys. Lett.* 1996, **256**, 454-464.
10. N. M. O'Boyle, A. L. Tenderholt and K. M. Langner, *J. Comput. Chem.* 2008, **29**, 839-845.
11. S. Cho, M.-C. Yoon, J. M. Lim, P. Kim, N. Aratani, Y. Nakamura, T. Ikeda, A. Osuka and D. Kim, *J. Phys. Chem. B.* 2009, **113**, 10619-10627.